GSA Data Repository 2019373

Palmer, M.R., et al., 2019, A short, sharp pulse of potassium-rich volcanism during continental collision and subduction: Geology, v. 47, https://doi.org/10.1130/G45836.1

A short, sharp pulse of potassium-rich volcanism during continental collision and subduction

SUPPLEMENTARY FILE

ANALYTICAL METHODS

The analytical method for determining the boron concentration and isotope composition of the samples has been adapted from Wei et al. (2013). All the reagents used were high purity and all the sample processing took place in clean laboratories equipped with boron-free HEPA filters at the University of Southampton.

Approximately 100 mg of rock powder was accurately weighed and transferred into a 7 ml screw top PFA vial, together with 100 μL of 1% mannitol, 100 μL H_2O_2 and 1 mL 24 M HF. The vial was sealed and placed on a hot plate for 3 days at 60^{o}C. A white precipitate, consisting largely of fluorite, was present in the sample solution after this time. Dissolution of this precipitate and analysis by inductively coupled plasma mass spectrometry (ICP-MS) revealed that it did not contain any detectable boron, in accordance with previous observations (Nakamura et al., 1992; Wei et al., 2013). After dissolution, 0.5 mL of the sample was added to 1.5 mL of water in a polypropylene centrifuge tube. After centrifuging, the supernatant was transferred to another 7 mL PFA vial and a further 2 mL of water was added to yield a 3 M HF solution.

The boron concentration was determined by taking 0.1 mL of the 3 M HF sample solution and diluting to 5 mL with 3% HNO_3 containing a 10 ng/g Be internal standard. The boron concentration was then determined using a Thermo Element high-resolution (HR) ICP-MS against a range of 0 to 5 ng/g boron standards (also containing 10 ng/g Be).

Boron was separated from the solution using Bio-Rad AG MP-1 anion exchange resin. The columns consisted of a polypropylene funnel fitted with a porous frit. A fresh aliquot of ~100 μL of resin was loaded into the stem of the funnel for each separation. The overall ion exchange chromatography procedure is summarized in Table DR1. The sample load volume was adjusted so that ~100 ng of boron was added to the column. The boron fraction was collected in a 7 mL PFA vial to which 10 μL of 1% mannitol was added and the solution was evaporated to dryness at 55°C.

The sample was taken up in 0.5 mL of 0.5 M HNO_3 to yield a solution with ~200 ng/g boron. Boron isotope analyses were then carried out using a Thermo Neptune multi-collector (MC) ICP-MS following the method described in Foster (2008) that was modified with the use of a 0.3 M HF/0.5 M HNO_3 wash solution to speed up the wash-out time. The NIST SRM 951 boric acid standard (200 ng/g) was used during the sample-standard bracketing and to define the $\delta^{11}B$ values of the samples. Typical in-run 2σ precisions were <0.2 ‰.

During this study, all samples were analyzed in batches of 10. Each batch consisted of duplicates of 4 powdered rock samples, a powdered rock reference material and a blank. Thus each sample was independently analyzed for both its concentration and $\delta^{11}B$ value at least twice, and 7 samples were analyzed in triplicate. The blank after sample dissolution was always <0.5 ng and typically <0.1 ng. The blank associated with the ion exchange chromatography was always <1 ng of boron and typically <0.3 ng (compared to a sample analyte of ~100 ng of boron). The largest difference between the highest and lowest $\delta^{11}B$ replicate analyses of a sample was 1.0 ‰, with the average difference being 0.3 ‰ (Table DR2). The largest difference between the highest and lowest boron concentration [B] replicate analyses of a sample was 10.7 % of the absolute value, with the average difference being 3.7 %. During this study, 10 analyses of standard IAEA-B5 (basalt from Etna volcano; Gonfiantini et al., 2003) yielded an average $\delta^{11}B$ value of -4.2 ± 0.2 ‰ (2σ) and an average

[B] of 9.2 ± 0.2 μg/g (2σ). These values compare well with values previously obtained for this reference material (Table DR3).

In addition to the 42 $\delta^{11}B$ and [B] data listed in Table 2, Tonarini et al. (2005) report data for 16 WA volcanic rocks. They did not analyse the IAEA-B5 reference material, but they report a $\delta^{11}B$ value of 7.3 ± 0.4 ‰ for the GSJ-JB2 basalt reference material. Four analyses of this reference material in this study yielded average $\delta^{11}B$ and [B] values of 7.2 ± 0.2 ‰ and 29.4 ± 0.7 μg/g, respectively. Hence, the $\delta^{11}B$ values within the two data sets are directly comparable.

ADDITIONAL REFERENCES CITED

Berryman, E.J., Kutzschbach, M., Trumbull, R.B., Meixner, A., van Hinsberg, V., Kasemann, S.A., and Franz, G., 2017, Tourmaline as a petrogenetic indicator in the Pfitsch Formation, Western Tauern Window, Eastern Alps: Lithos, v. 284-285, p. 138-155, doi: 10.1016/j.lithos.2017.04.008.

Foster, G.L., 2008, Seawater pH, pCO_2 and [CO_3^{2-}] variations in the Caribbean Sea over the last 130 kyr: A boron isotope and B/Ca study of planktic foraminifera: Earth and Planetary Science Letters, v. 271, p. 254-266, doi:10.1016/j.epsl.2008.04.015.

Gonfiantini, R., and 30 others, 2003, Intercomparison of boron isotope and concentration measurements. Part II: Evaluation of results: Geostandards Newsletter, v. 27, p. 41-57, doi:10.1111/j.1751-908X.2003.tb00711.x.

Hansen, C.T., Meixner, A., Kasdemann, S.A., and Bach, W., 2017, New insight on Li and B isotope fractionation derived from batch reaction investigations: Geochimica et Cosmochimica Acta, v. 217, p. 51-79, doi: 10.1016/j.gca.2017.08.014 0016-7037/2017.

Nakamura, E., Ishikawa, T., Birck, J.L., and Allegre, C.J., 1992, Precise boron isotopic analysis of natural rock samples using a boron-mannitol complex: Chemical Geology, v. 94, p. 193-204, doi:10.1016/0168-9622(92)90012-Y.

Pi, J.L., You, C.F., Chung, C.H., Micro-sublimation separation of boron in rock samples for isotopic measurement by MC-ICP-MS. Journal of Analytical Atomic Spectrometry, 29, 861-867, DOI: 10.1039/c3ja50344e

Romer, R.L., Meixner, A., and Hahne, K., 2014, Lithium and boron isotopic composition of sedimentary rocks- The role of source history and depositional environment: A 250 Ma record from the Cadomian orogeny to the Variscan orogeny: Gondwana Research, v. 26, p. 1093-1110, doi: 10.1016/j.gr.2013.08.015.

Wei, G., Wei, J., Liu, Y., Ke, T., Ren, Z., Ma, J., and Xu, Y., 2013, Measurement on high-precision boron isotope of silicate materials by a single column purification method and MC-ICP-MS: Journal of Analytical Atomic Spectrometry, v. 28, p. 606-612, doi: 10.1039/C3JA30333K.

FIGURE CAPTIONS

Figure DR1.

Harker diagrams for WA volcanic rocks

(a) [B] μg/g vs. SiO_2 wt%, (b) [B] μg/g vs. MgO wt%, (c) $\delta^{11}B$ ‰ vs. SiO_2 wt%, (d) $\delta^{11}B$ vs. MgO wt%. Major element data from Ersoy and Palmer (2013), and references therein.

Figure DR2.

[B] and $\delta^{11}B$ values versus radiogenic isotope ratios

(a) [B] μg/g vs $^{87}Sr/^{86}Sr$, (b) $\delta^{11}B$ ‰ vs $^{87}Sr/^{86}Sr$, (c) $\delta^{11}B$ ‰ vs $^{143}Nd/^{144}Nd$, (d) $\delta^{11}B$ ‰ vs $^{208}Pb/^{204}Pb$. Radiogenic isotope data from Ersoy and Palmer (2013), and references therein.

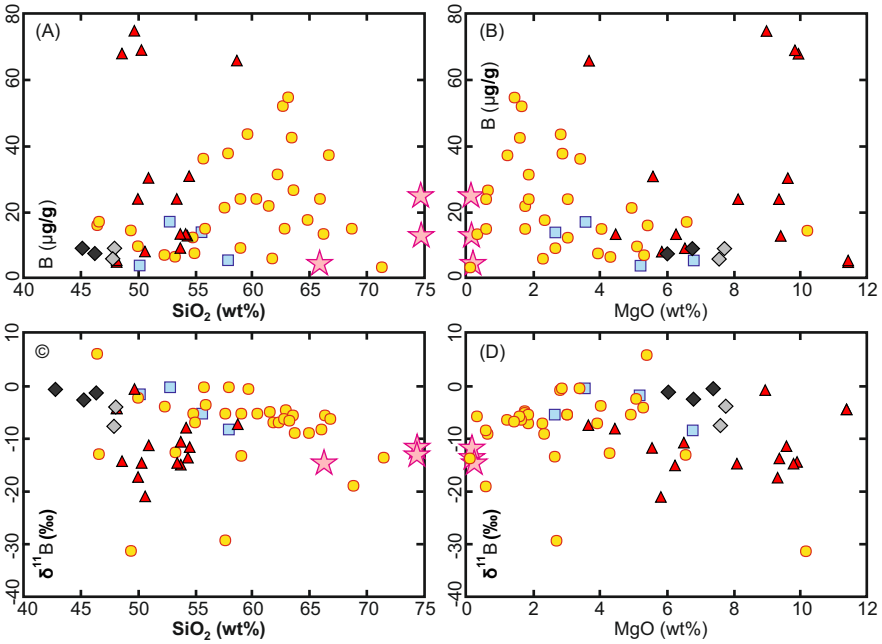

Figure DR1

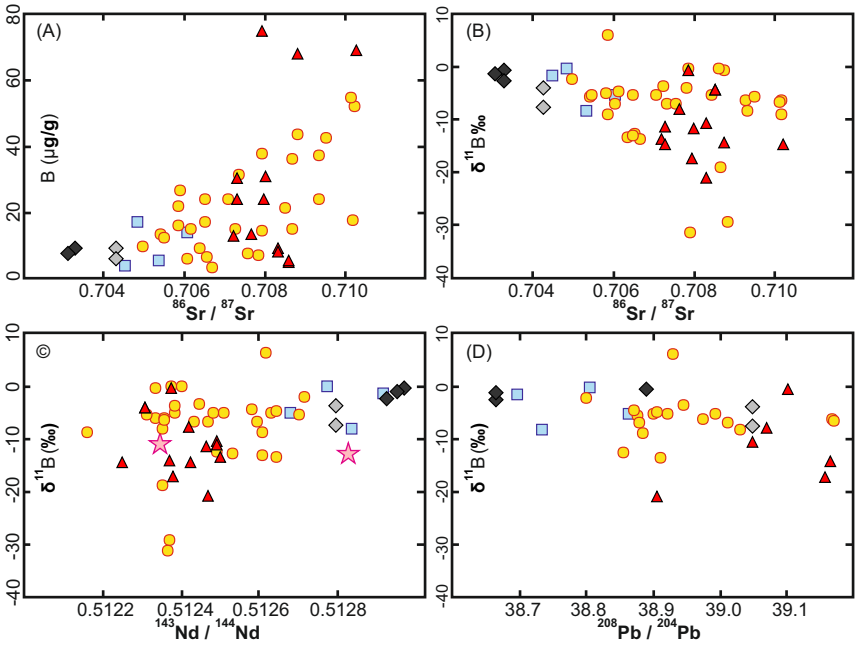
(A)
B (µg/g)
0
20
40
60
80
0.704
0.706
0.708
0.710
86Sr / 87Sr
(B)
δ11B ‰
10
0
-10
-20
-30
-40
0.704
0.706
0.708
0.710
86Sr / 87Sr
©
δ11B (‰)
10
0
-10
-20
-30
-40
0.5122
0.5124
0.5126
0.5128
143Nd / 144Nd
(D)
δ11B (‰)
10
0
-10
-20
-30
-40
38.7
38.8
38.9
39.0
39.1
208Pb / 204Pb

Figure DR2

Table DR1
Ion exchange chromatography procedure

Step	Operation
Step 1	Resin washing and conditioning
	2.5 mL H_2O
	0.5 mL 24 M HF
	1.5 mL H_2O
Step 2	Sample loading
	3 M HF (volume adjusted according to sample)
Step 3	Matrix elution
	2 x 0.5 mL H_2O
	8.5 mL 0.1 M HCl
Step 4	Boron collection
	1.2 mL 24 N HF

Table DR2.
Boron concentration and isotope data for samples analysed in this study (UTM coordinates give sample location)

	B concentration (μg/g)				δ^{11}B (‰)			
Sample (UTM)	**1st run**	**2nd run**	**3rd run**	**mean**	**1st run**	**2nd run**	**3rd run**	**mean**
Early Eocene orogenic								
(Kizderbent volcanics)								
G5 (0651592/4488750)	5.2	5.1		**5.2**	-8.3	-8.3		**-8.3**
G28 (0651592/4488750)	16.9	16.8	16.6	**16.8**	-0.6	-0.5	0.2	**-0.3**
G45 (0749558/4499472)	3.8	3.7		**3.8**	-1.7	-1.6		**-1.6**
G48 (0737486/4502470)	14.2	13.6	13.9	**13.9**	-5.2	-5.3	-5.7	**-5.4**
Middle Eocene – Miocene orogenic								
(Late Eocene Balıklıçeşme volcanics)								
B5 (0492827/4448313)	16.1	16.3	16.0	**16.1**	6.3	6.2	5.8	**6.1**
B11 (0500469/4459685)	12.9	13.3		**13.1**	-5.5	-5.8		**-5.7**
B12 (0486130/4466913)	14.6	14.9		**14.7**	-4.6	-4.7		**-4.7**
B17 (0473433/4454350)	23.1	24.0	23.7	**23.6**	-5.7	-5.3	-4.8	**-5.3**
B35 (0485295/4455090)	9.9	9.3		**9.6**	-2.2	-2.2		**-2.2**
C15 (0481003/4413380)	6.4	6.0		**6.2**	-12.6	-13.1		**-12.8**
C42 (0466010/4432014)	6.2	5.6		**5.9**	-7.0	-7.3		**-7.1**
(Oligocene Kirazlı volcanics)								
B21 (0477628/4444050)	3.4	3.4		**3.4**	-13.7	-13.5		**-13.6**
C7 (0480017/4430858)	11.9	12.0		**12.0**	-5.2	-5.2		**-5.2**
C9 (0477916/4420541)	14.6	14.4	14.7	**14.6**	-3.8	-3.7	-4.1	**-3.8**
C31 (0497168/4425055)	26.5	26.7		**26.6**	-8.9	-9.4		**-9.1**
C36 (0474152/4433482)	21.0	21.9		**21.5**	-5.1	-4.8		**-5.0**
(Oligocene Hallaçlar volcanics)								
HG2 (0530735/4407610)	31.0	31.1		**31.1**	-6.8	-7.0		**-6.9**
HG9 (0536865/4436733)	24.0	24.3	23.9	**24.1**	-5.0	-5.4	-5.1	**-5.2**
(Oligocene Keşan volcanics)								
K20 (0469494/4521168)	8.5	9.4		**9.0**	-13.2	-13.2		**-13.2**
(Miocene Yuntdağı volcanics)								

129 (0540981/4353496)	15	14.3		**14.7**	-19.1	-19.1	5.8	**-19.1**
(Miocene Yağcıdağ volcanics)								
510 (0657381/4302983)	49.7	54.6		**52.1**	-6.1	-6.3		**-6.2**
YF2 (0657381/4302983)	53.5	55.4	54.1	**54.3**	-6.6	-6.5	-6.3	**-6.5**
(Miocene Eğreltidağ volcanics)								
521 (0657795/4308366)	25.1	23.1		**24.1**	-8.6	-8.1		**-8.4**
(Miocene Sevinçler volcanics)								
718 (0652561/4322172)	36.7	37.4		**37.1**	-6.4	-6.4		**-6.4**
(Miocene Miocene Asitepe volcanics)								
754 (0636380/4309275)	42.8	42.1		**42.5**	-5.7	-5.3		**-5.5**
(Miocene Yaylaköy volcanics)								
L36 (0453515/4270500)	21.7	20.5		**21.1**	-5.6	-5.8		**-5.4**
(Miocene Armağandağ volcanics)								
L47 (0451794/4236840)	43.7	43.2		**43.5**	-0.8	-0.8		**-0.8**
(Miocene Kuzayır lamproite)								
518 (0660886/4311660)	9.1	9.3		**9.2**	-11.2	-10.2		**-10.7**
528 (0660886/4311660)	8.2	7.8		**8.0**	-20.8	-21.2		**-21.0**
(Miocene Doğanca lamproite)								
K17 (0475167/4528879)	4.8	5.1		**5.0**	-4.0	-4.4		**-4.2**
K17B (0475167/4528879)	4.9	5.4		**5.2**	-4.3	-4.1		**-4.2**
(Miocene Kayacık volcanics)								
756 (0601705/4305141)	16.7	18.0		**17.4**	-9.1	-8.8		**-8.9**
(Miocene Güre lamproite)								
822 (0679728/4281490)	66.2	71.2		**68.7**	-14.7	-14.8		**-14.7**
(Miocene Karaburun volcanics)								
L30 (0458200/4275780)	14.1	14.7		**14.4**	-31.4	-31.3		**-31.3**
(Miocene Orhanlar basalt)								
536 (0680006/4311835)	24.5	23.7		**24.1**	-17.2	-17.4		**-17.3**
541 (0679810/4310909)	67.3	68.5		**67.9**	-14.7	-14.2		**-14.4**
543 (0679836/4310901)	72.8	76.7		**74.8**	-0.5	-1.0		**-0.8**
(Miocene Naşa basalt)								

746 (0671372/4333717)	13.4	13.6	**13.5**	-8.0	-8.2		**-8.1**
Transitional – Miocene (Late Miocene Kabaklar basalt)							
520-1 (0671542/4298101)	5.9	5.7	**5.8**	-7.4	-7.6	-4.8	**-7.5**
Basement Rocks (Menderes Massif - gneiss)							
G01 (0673572/4300943)	13.4	13.1	**13.3**	-13.3	-12.9		**-13.1**
G02 (0673572/4300943)	24.9	26.7	**25.8**	-11.3	-10.8		**-11.0**
(Menderes Massif - Rahmanlar granite)							
Y23-2 (0674406/4302063)	4.1	4.4	**4.3**	-14.1	-15.1		**-14.6**

Table DR3.
Boron concentration and isotope data for IAEA-B5 reference material

Source	[B] (μg/g) ± 2σ	$\delta^{11}B$ (‰)± 2σ
This study	9.2 ± 0.2	-4.2 ± 0.2
Gonfiantini et al., 2003	10.0 ± 1.2	-4.1 ± 2.7
Pi et al., 2014	9.3 ± 0.1	-3.9 ± 0.2
Romer et al., 2014	10.0 ± 1.0	-3.7 ± 0.7
Hansen et al., 2017		-4.3 ± 0.2
Berryman et al., 2017	9.3 ± 0.4	-4.3 ± 0.2